First-Principles Calculation of the 17 O NMR Parameters in Ca Oxide and Ca Aluminosilicates: the Partially Covalent Nature of the Ca–O Bond, a Challenge for Density Functional Theo…

ARTICLE *in* JOURNAL OF THE AMERICAN CHEMICAL SOCIETY · NOVEMBER 2004

Impact Factor: 12.11 · DOI: 10.1021/ja0490830 · Source: PubMed

4 AUTHORS, INCLUDING:

Magali Benoit

Centre d'Élaboration de Matériaux et d'Etud…

38 PUBLICATIONS **992** CITATIONS

SEE PROFILE

J|A|C|S
ARTICLES
Published on Web 09/08/2004

First-Principles Calculation of the ^{17}O NMR Parameters in Ca Oxide and Ca Aluminosilicates: the Partially Covalent Nature of the Ca−O Bond, a Challenge for Density Functional Theory

Mickaël Profeta,[†] Magali Benoit,*[,‡] Francesco Mauri,[†] and Chris J. Pickard[§]

Contribution from the Laboratoire de Minéralogie-Cristallographie de Paris, Université Pierre et Marie Curie, 4, place Jussieu, 75252 Paris Cedex, France; Laboratoire des Verres, cc 69, Université Montpellier II, Place E. Bataillon, 34095 Montpellier Cedex 5, France; and TCM Group, Cavendish Laboratory, Madingley Road, Cambridge, CB3 OHE, United Kingdom

Received February 18, 2004; E-mail: magali.benoit@ldv.univ-montp2.fr

Abstract: We apply density functional theory (DFT) to the calculation of the ^{17}O NMR parameters in Ca and Mg oxides and aluminosilicates. We study the accuracy of the Perdew, Burke, and Ernzerhof (PBE) generalized-gradient approximation to DFT in the description of these systems and the origin of the experimentally observed large dependence of the ^{17}O chemical shift on the alkaline earth ion. We find that (i) the partially covalent nature of the Ca−O bond has a huge impact on the O chemical shifts. The Ca−O covalence alone explains why in Ca oxides and aluminosilicates the ^{17}O chemical shifts are much more deshielded than those of the corresponding Mg compounds. (ii) The Ca−O covalence is overestimated by the PBE functional. Thus PBE-DFT is not able to reproduce the measured ^{17}O NMR parameters in Ca oxide and Ca aluminosilicates. (iii) It is possible to correct for the PBE-DFT deficiency in a simple and transferable way and to predict very accurate ^{17}O NMR parameters. Such accuracy allows us to assign the ^{17}O NMR spectra of two important model systems: the grossite aluminate ($CaAl_4O_7$) and the wollastonite ($CaSiO_3$) silicate.

Introduction

The study of aluminosilicates is central to a wide range of fundamental and applied scientific disciplines. Indeed, the aluminosilicates represent a large class of natural and technological materials that includes minerals, zeolites, ceramics, concretes, glasses, and melts. These systems can contain, besides Al, Si, and O, alkaline and alkaline-earth cations such as Na^+, K^+, Mg^{2+}, and Ca^{2+}.

Nuclear magnetic resonance spectroscopy (NMR) is an important analytic technique for the study of the microscopic atomistic structure and processes in aluminosilicate systems. NMR spectroscopy of ^{29}Si and ^{27}Al is commonly used. More recently, advances in multidimensional NMR for quadrupolar nuclei, the availability of higher field spectrometers, and isotopic enrichment have promoted the use of ^{17}O as an active NMR nucleus in the study of aluminosilicates (see, for example, refs 1−3).

The interpretation of ^{17}O NMR spectra of complex aluminosilicate systems (glasses, disordered zeolites, and complex minerals) can be extremely challenging. NMR spectra are usually interpreted by comparison with the spectra of simple, well characterized, prototype materials. However, ^{17}O isotopic enrichment requires the synthesis of enriched samples of these prototype materials, and this synthesis can be expensive and complex. Moreover, when more than one inequivalent site is present, the assignment of each individual NMR ^{17}O peak to a crystallographic O site is not trivial, even in simple prototype materials.[2−5]

To assist the interpretation of ^{17}O NMR spectra, it would be very helpful to be able to reliably compute the NMR parameters of a model system for which we can precisely control all the atomic positions. The calculation of NMR parameters from first principles has recently become possible for large infinite solids described within periodic boundary conditions, plane wave basis sets, and density functional theory (DFT). In particular, the electric field gradients and the NMR chemical shifts can be computed using the projector augmented wave (PAW) method[6−8] and the gauge-including projector augmented wave (GIPAW) method,[8,9] respectively. In these approaches the only significant source of error is the use of approximated exchange-correlation DFT functionals. Alternatively, the NMR parameters can be predicted by modeling the infinite solids as finite clusters and using atomic orbital basis sets[2,10−13]. However, the use of finite

[†] Université Pierre et Marie Curie.
[‡] Université Montpellier II.
[§] Cavendish Laboratory.

(1) Stebbins, J. F.; Xhu, Z. *Nature* **1997**, *60*, 390. Farnan, I. *Nature* **1997**, *390*, 14.
(2) Bull, L. M.; Bussemer, B.; Anupold, T.; Reinold, A.; Samoson, A.; Sauer, J.; Cheetham, A. K.; Dupree, R. *J. Am. Chem. Soc.* **2000**, *122*, 4948.
(3) Bull, L. M.; Cheetham, A. K.; Anupold, T.; Reinold, A.; Samoson, A.; Sauer, J.; Bussemer, B.; Lee, Y.; Gann, S.; Shore, J.; Pines, A.; Dupree, R. *J. Am. Chem. Soc.* **1998**, *120*, 3510.
(4) Stebbins, J. F.; Oglesby, J. V.; Kroeker, S. *Am. Mineral.* **2001**, *86*, 1307.
(5) Mueller, K. T.; Baltisberger, J. H.; Wooten, E. W.; Pines, A. *J. Phys. Chem.* **1992**, *96*, 7001.
(6) Blöchl, P. E. *Phys. Rev. B* **1994**, *50*, 17953.
(7) Petrilli, H. M.; Blöchl, P. E.; Blaha, P.; Schwarz, K. *Phys. Rev. B* **1998**, *57*, 14690.
(8) Profeta, M.; Mauri, F.; Pickard, C. J. *J. Am. Chem. Soc.* **2003**, *125*, 541.
(9) Pickard, C. J.; Mauri, F. *Phys. Rev. B* **2001**, *63*, 245101.

10.1021/ja0490830 CCC: $27.50

clusters introduces, in addition to the DFT errors, other sources of inaccuracy that are difficult to control and to fully eliminate.

The PAW and GIPAW approaches to the simulation of the ^{17}O NMR parameters have already been applied to the study of the pure silicates[8] and Na silicates[14] with very good results, even for large (up to 144 atoms in a unit cell) complex structures such as the zeolites or Na silicate glasses. In particular, these results show that the approximate PBE-DFT functional[15] reproduces the experimental ^{17}O NMR parameter in pure SiO_2 and Na_2O-SiO_2 phases very well.

Given these results, one might expect that the ^{17}O NMR parameters of Ca aluminosilicates would also be well described within the PBE-DFT approximation. Indeed, in current models of the Ca aluminosilicates, the Ca−O bonds are considered to be mostly ionic with the Ca atoms acting as charge compensators for the presence of nonbridging oxygens and of $Al(O_{0.5})_4^-$ tetrahedra, as do the Na atoms in the Na aluminosilicates. However, this picture has been challenged by recent work on alkaline-earth oxides where the partially covalent nature of the Ca−O bond has been observed.[16] Moreover, a pure ionic bond between O and the alkaline or alkaline-earth metal can hardly explain the huge dependence of ^{17}O chemical shift on the species of the alkaline or alkaline-earth atom. For example, the ^{17}O chemical shifts of nonbridging O are found to be approximately 40 ppm in the Na aluminosilicates,[14,17] 75 ppm in the K aluminosilicates,[17] 40 ppm in the Mg aluminosilicates,[18,19] and 105 ppm in the Ca aluminosilicates.[5] The dependence on the alkaline-earth atom is even larger in simple oxides: the ^{17}O chemical shift of MgO being 47 ppm and that of CaO being 294 ppm.

In this paper, we apply the PAW and GIPAW methods to the crystalline calcium aluminosilicates, so as (i) to establish the reliability of the PBE-DFT approximation for the description of ^{17}O NMR parameters in such systems and (ii) to determine the origin of the dependence of the ^{17}O chemical shift on the species of the alkaline or alkaline-earth atom.

Details of the NMR Parameter Calculation

The NMR shielding tensor, $\bar{\sigma}(\mathbf{r})$ is defined as $\mathbf{B_{in}}(\mathbf{r}) = \bar{\sigma}(\mathbf{r})\mathbf{B}$, where $\mathbf{B}$ is an external uniform magnetic field and $\mathbf{B_{in}}(\mathbf{r})$ is the induced nonuniform magnetic field. The isotropic shielding $\sigma(\mathbf{r})$ is one-third of the trace of the shielding tensor and the isotropic chemical shift $\delta(\mathbf{r})$ for a nucleus in the position $\mathbf{r}$ is defined as

$$\delta(\mathbf{r}) = -[\sigma(\mathbf{r}) - \sigma^{\mathrm{ref}}] \tag{1}$$

where σ^{ref} is the isotropic shielding of the same nucleus in a reference system. For ^{17}O the reference is a spherical liquid water sample, for ^{29}Si it is a spherical liquid sample of tetramethylsilane, and for ^{27}Al it is a spherical sample of 1 M acidified aqueous solution of $Al(NO_3)_3$. The values of δ are given in ppm.

Table 1. Relaxed Coordinates of Berlinite, $AlPO_4$[a]

	x	y	z
P	0.464 69	0.000 00	0.500 00
O1	0.418 07	0.292 97	0.064 20
O2	0.411 73	0.257 54	0.550 72
Al	0.466 55	0.000 00	0.000 00

[a] The theoretical lattice constants (before rescaling) obtained by PBE-DFT relaxation are $a = b = 4.991$ Å, $c = 11.080$ Å, $\alpha = \beta = 90°$, $\gamma = 120°$

Nuclei with a spin of greater than $^1/_2$ have quadrupolar parameters related to the traceless electric field gradient (EFG) $\bar{G}(\mathbf{r})$,

$$G_{\alpha\beta}(\mathbf{r}) = \frac{\partial E_\alpha(\mathbf{r})}{\partial r_\beta} - \frac{1}{3}\delta_{\alpha\beta}\sum_\gamma \frac{\partial E_\gamma(\mathbf{r})}{\partial r_\gamma} \tag{2}$$

where α,β,γ denote the Cartesian coordinates x, y, z and $E_\alpha(\mathbf{r})$ is the local electric field at position $\mathbf{r}$. If the eigenvalues of the EFG tensor are labeled V_{xx},V_{yy},V_{zz} so that $|V_{zz}| > |V_{yy}| > |V_{xx}|$, then one can define the quadrupolar coupling constant as

$$Cq = \frac{eQV_{zz}}{h} \tag{3}$$

and the asymmetry parameter as

$$\eta = \frac{V_{xx} - V_{yy}}{V_{zz}} \tag{4}$$

where e is the absolute value of the electron charge, h is the Planck constant, and Q is the nuclear quadrupolar moment. Finally, the constant Pq is equal to $Cq(1 + \eta^2/3)^{1/2}$. The values of Cq and Pq are given in MHz.

We obtain absolute shielding tensors from our calculations. To fix the ^{17}O δ-scales we use for σ^{ref} the value of 261.5 ppm, which has been obtained in ref 8 by comparing the experimental and theoretical chemical shifts in various SiO_2 systems. To compute the Cq for ^{17}O, we use the experimental quadrupolar moment $Q = 2.5510^{-30}$ m^2. For ^{29}Si, by imposing the constraint that the calculated value of δ in quartz should match the experimental one,[20] we find that $\sigma^{\mathrm{ref}} = 335.15$ ppm. For ^{27}Al, by ensuring that the calculated value of δ for the Al site in berlinite matches the experimental one, we find that $\sigma^{\mathrm{ref}} = 556.1$ ppm. Berlinite is an $AlPO_4$ crystal with a structure similar to that of quartz, where silicon atoms are alternately replaced by Al or P atoms.[21] Since the calculated forces on the atoms of the experimental structure[21] are large, for the NMR calculation we relax the internal coordinates and cell parameters within the PBE-DFT framework. The relaxed structure is reported in Table 1. To take into account systematic errors in the PBE-DFT description of bond lengths in the NMR calculations, we rescale the resulting lattice parameters by 99.0% so as to match the experimental volume. The calculated absolute shielding constants and the experimental chemical shifts[22] are presented in Table 2. Finally, for the calculation of the Cq of ^{27}Al,

(10) Tossell, J. A.; Lazzaretti, P. *Chem. Phys.* **1987**, *112*, 205.
(11) Xue, X.; Kanzaki, M. *J. Phys. Chem. B* **1999**, *103*, 10816.
(12) Kubicki, J. D.; Toplis, M. J. *Am. Mineral.* **2002**, *87*, 668.
(13) Tossell, J. A. *Phys. Chem. Miner.* **2004**, *31*, 41.
(14) Charpentier, T.; Ispas, S.; Profeta, M.; Mauri, F.; Pickard, C. J. *J. Phys. Chem. B* **2004**, *108*, 4147.
(15) Perdew, J. P.; Burke, K.; Ernzerhof, M. *Phys. Rev. Lett.* **1996**, *77*, 3865.
(16) Posternak, M.; Baldereschi, A.; Kakauer, H.; Resta, R. *Phys. Rev. B* **1997**, *55*, R15983.
(17) Xue, X.; Stebbins, J. F.; Kanzaki, M. *Am. Mineral.* **1994**, *79*, 31.
(18) Kyung, H.; Timken, C.; Schramm, S. E.; Kirkpatrick, R. J.; Oldfield, E. *J. Chem. Phys.* **1987**, *91*, 1054.
(19) Mueller, K. T.; Wu, Y.; Chmelka, B. F.; Stebbins, J.; Pines, A. *J. Am. Chem. Soc.* **1991**, *113*, 32.
(20) The Si pseudopotential in this paper is different from that used in ref 8. This explains the slightly different values of σ^{ref} (337.3 ppm) used in ref 8.
(21) Wyckoff. *Crystal structures*; John Wiley: New York; Vol. 3, p 31.
(22) Bleam, W. F.; Pfeffer, P. E.; Frye, J. S. *Phys. Chem. Miner.* **1989**, *16*, 45.

Table 2. Experimental[22] Chemical Shifts (δ) and Calculated Absolute Shielding Constants (σ) of Berlinite

nuclei	experiment δ	theory σ
P	−24.5	325.2
O1		193.4
O2		194.4
Al	44.5	511.6

we use the experimental nuclear quadrupolar moment $Q = 14.010^{-30}$ m^2.

The calculations are performed within density functional theory (DFT). We use the PBE generalized gradient approximation in all of our calculations,[15] which gives very similar results to those obtained using the PW91 approximation[23] and corrects some of the numerical instabilities. The core−valence interactions are described by Troulier−Martins norm conserving pseudopotentials[24] in the Kleinman−Bylander[25] form, with s nonlocality for O, and s and p nonlocality for Si, Al, P, Mg, and Ca. The core for O and Mg is $1s^2$, and for Si, Al, P, and Ca it is $1s^22s^22p^6$. The core radii are 2.0 a.u. for Si, Al, P and 1.45 a.u. for O. For Mg they are 1.6 a.u., 1.0 a.u. and 2.0 a.u. for the s, p and d channels, respectively, and for Ca they are 1.45 a.u., 2.0 a.u. and 1.45 a.u. for the s, p and d channels, respectively. The structures are described as infinite periodic solids using periodic boundary conditions. The wave functions are expanded in a set of plane waves with a kinetic energy cutoff of 140 Ry for MgO and 80 Ry for all the other structures. Integrals over the Brillouin zone are performed using $4 \times 4 \times 4$ Monkhorst−Pack grids[26] for berlinite, CaO, and MgO and a $2 \times 2 \times 2$ grid for wollastonite. For grossite we use a $2 \times 2 \times 2$ grid for the charge density and EFG calculation and a $4 \times 4 \times 4$ grid for the NMR calculation.

To compute the shielding tensor using pseudopotentials we use the GIPAW[9] approach. This permits the results of fully converged all-electron calculations to be reproduced. To compute the EFG tensors, we use a PAW approach to reconstruct the all-electron results.[6−8] For both the PAW and GIPAW calculations, we use two projectors in each of the s, p, and d angular momentum channels. This approach has previously been successfully applied to the calculation of the ^{17}O parameters in SiO_2 polymorphs, including zeolites,[8] and of Na_2O-SiO_2 crystalline and amorphous systems.[14]

Breakdown of PBE-DFT for Ca

We compute the NMR chemical shift and quadrupolar parameters for lime (CaO), grossite ($CaAl_4O_7$), and wollastonite ($CaSiO_3$) crystals, three structures for which experimental NMR data have been previously measured.[4,5,27] Calcium oxide (lime) has a cubic structure.[28] We also perform calculations for periclase (MgO), which has the same structure as lime, to compare the influence of an alkaline-earth ion on the ^{17}O chemical shift. In grossite and wollastonite all the Si and Al atoms are situated at the center of AlO_4 and SiO_4 tetrahedra. The structure of grossite, Figure 1, contains three inequivalent bridging oxygens (O1, O2, and O3) linked with two Al atoms and one oxygen tricluster (O4) linked with three Al atoms. Since the forces on the atoms computed for the experimental structure of grossite[29] are significant, we relax the internal coordinates and cell parameters within the PBE-DFT framework. To take into account systematic errors in the PBE-DFT description of bond lengths in the NMR calculations, we rescale the resulting lattice parameters by 98.6% so as to match the experimental volume. The relaxed atomic coordinates of grossite are presented in Table 3. For wollastonite, Figure 1, we consider the 2M structure[30] which contains three bridging oxygen atoms (OC1, OC2, and OC3) and six nonbridging oxygen atoms whose charge is compensated by three calcium ions. For wollastonite, lime, and periclase, the NMR parameter calculations are performed for the experimental structures.

The PBE-DFT ^{17}O NMR parameters of the periclase, lime, grossite, and wollastonite crystals are presented in Table 4. For comparison, we include in the table the experimental NMR parameters (the assignment of these parameters to crystallographic sites is discussed in section 5). The computed electric field gradients are in good agreement with the experimental ones. In contrast, there are substantial discrepancies between the computed and measured chemical shifts. The differences between theory and experiments are about 124 ppm for CaO, 20 ppm for sites O1 to O3 in grossite, and 30 ppm for sites OA1 to OB3 in wollastonite. For the other sites (O4 in grossite; OC1, OC2, and OC3 in wollastonite), the differences between theory and experiment are about 5 ppm. This is surprising, since previous results for SiO_2 and Na_2O-SiO_2 systems[8,14] have demonstrated good accuracy for the calculation of ^{17}O chemical shifts, with typical errors of less than 5 ppm. Interestingly, the sites with the largest errors are the ones closest to the calcium atoms: the bridging oxygens in grossite and the nonbridging oxygens in wollastonite. Finally, as shown in Table 4, in MgO the discrepancy with experiment[27] is less than 12 ppm, 1 order of magnitude smaller than the error in CaO. These results suggest that the presence of Ca, in particular, in these GGA-PBE calculations adversely affects the prediction of NMR chemical shifts (but not the EFGs) in these systems.

Improving on the DFT Results

The main difference between MgO and CaO is the presence of the unoccupied 3d orbitals of Ca near the occupied states. In the Ca−O bond, the Ca 3d orbitals can partially hybridize with the occupied 2p states. As a consequence, the Ca−O bond has an ionocovalent character that is absent in the purely ionic Mg−O bond. This contrasting behavior is observed in the experimental values of the oxygen Born effective charge (BEC) of crystalline MgO and CaO.

The BECs, also known as dynamical charges, are responsible for the infrared activity of vibrational modes. The BEC of an atom is defined as the derivative of the electric dipole per unit cell with respect to the displacement of the atom (in a zero macroscopic electric field). For purely ionic bonding, the electrons around an O would rigidly follow the O displacements, and the O BEC would be equal to the nominal value of −2.[16,31] In the presence of covalent bonding, in response to a displacement of an O atom toward a metal ion, a fraction of the O electrons would rigidly follow the O movement, but a different

(23) Perdew, J. P.; Wang, Y. *Phys. Rev. B* **1992**, *45*, 13244.
(24) Troulier, N.; Martins, J. L. *Phys. Rev. B* **1991**, *43*, 1993.
(25) Kleinman, L.; Bylander, D. *Phys. Rev. Lett.* **1982**, *48*, 1425.
(26) Monkhorst, H. J.; Pack, J. D. *Phys. Rev. B* **1976**, *13*, 5188.
(27) Turner, G. L.; Chung, S. E.; Oldfield, E. *J. Magn. Res.* **1985**, *64*, 316.
(28) Huang, Q.; et al. *Physica C* **1994**, *227*, 1.
(29) Goodwin, D. W.; Lindop, A. J. *Acta Crystallogr.* **1970**, *B26*, 1230.
(30) Ohashi, Y. *Phys. Chem. Miner.* **1984**, *10*, 217.
(31) See in particular Figure 2 of Ph. Ghosez, Michenaud, J.-P.; Gonze, X. *Phys. Rev. B* **1998**, *58*, 6224−6240.

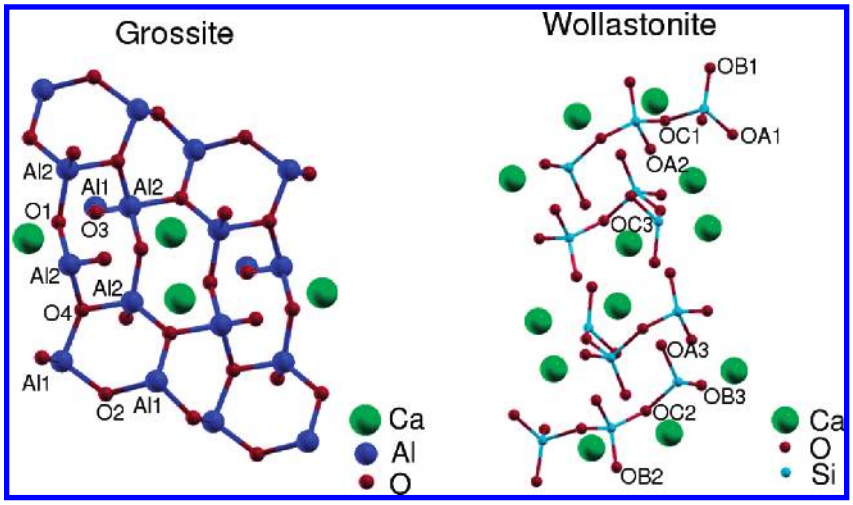

Figure 1. Three-dimensional models of the grossite (left) and wollastonite (right) structures.

Table 3. Relaxed Coordinates of Grossite, $CaAl_4O_7$[a]

	x	*y*	*z*
Ca	0.000 00	0.804 65	0.250 00
Al1	0.163 63	0.085 83	0.305 37
Al2	0.120 57	0.439 65	0.245 29
O1	0.000 00	0.530 14	0.250 00
O2	0.116 13	0.053 76	0.571 81
O3	0.119 01	0.254 26	0.150 21
O4	0.192 74	0.444 16	0.580 98

[a] The theoretical lattice constants (before rescaling) obtained by PBE-DFT relaxation are $a = 13.0055$ Å, $b = 8.9668$ Å, $c = 5.5055$ Å, $\alpha = 90°$, $\beta = 106.20°$, $\gamma = 90°$.

Table 4. ^{17}O NMR Parameters of Lime, Grossite, and Wollastonite[a]

	experiment			PBE-DFT			corrected PBE-DFT			
compound	δ	*Cq*	η	δ	*Cq*	η	δ	*Cq*	η	assign.
MgO	47.0	0.0	0.0	58.8	0.0	0.0				
CaO	294.0	0.0	0.0	418.05	0.0	0.0	294.04	0.0	0.0	
grossite	71.6	1.9	0.7	91.82	2.13	0.67	82.21	2.06	0.81	O1
	61.5	1.8	0.5	82.69	1.77	0.64	65.63	1.87	0.50	O2
	56.8	2.1	0.5	72.34	1.84	0.43	57.30	1.95	0.27	O3
	40.6	2.5	0.4	42.95	2.46	0.23	43.18	2.44	0.23	O4
	δ	*Pq*		δ	*Pq*	η	δ	*Pq*	η	assign.
wollastonite	115	2.3		153.11	2.42	0.18	115.29	2.52	0.19	OA1
	114	2.6		146.43	2.31	0.10	110.09	2.41	0.11	OA2
	107	2.2		138.88	2.26	0.07	103.89	2.30	0.21	OB2
	97	2.0		133.11	2.34	0.37	99.74	2.31	0.23	OB1
	103	2.9		136.90	3.01	0.40	103.51	3.10	0.38	OB3
	88	2.6		118.89	2.74	0.07	90.33	2.82	0.04	OA3
	75	4.8		82.69	4.91	0.53	78.04	4.92	0.49	OC2
	75	4.8		81.82	5.02	0.51	77.62	5.03	0.47	OC3
	67	4.7		71.61	4.90	0.10	70.95	4.98	0.09	OC1

[a] Comparison between experimental data and the results obtained with the original PBE-DFT Hamiltonian (PBE-DFT) and a corrected PBE-DFT Hamiltonian in which the position of Ca 3d orbitals is shifted by +3.2 eV (corrected PBE-DFT). The assignment is labeled with the same convention used in the description of crystalline structures.[29,30] The experimental NMR parameters are taken from refs 4, 5, and 27.

fraction would move from the O orbitals to the metal ion orbitals. In this case, the electron transfer from the O to the metal ion would increase the O BEC beyond its nominal value.[16,31] The O effective charges in MgO and in CaO are equal to -1.99 ± 0.03 and -2.28 ± 0.02,[32] respectively. As it is clearly shown in ref 16, the deviation from the nominal value in CaO is due to the Ca-3d O-2p hybridization.

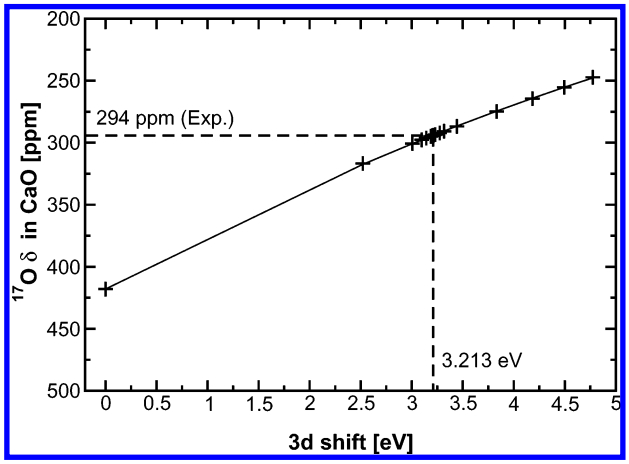

Figure 2. ^{17}O chemical shift in CaO (lime) calculated with a PBE-DFT Hamiltonian in which the Ca 3d orbital is shifted by a constant value. The ^{17}O chemical shift is plotted as a function of the Ca 3d shift. The 3d shift is defined for an isolated Ca^{2+} ion. The crosses are the calculated points, and the line is a guide for the eye. For a shift of 3.2 eV, the calculated ^{17}O chemical shift matches the experimental one.

To study the impact of this hybridization on the ^{17}O chemical shifts, we follow the approach of ref 16. We artificially adjust the energy level of the Ca 3d orbitals in the calculation. To do this, we simply modify the d channel of the Ca pseudopotential. We shift the potential inside the core region ($r < 2.0$ au) by a constant and otherwise leave the potential outside unmodified. By varying the value of this constant, we change the energy level of the 3d Ca orbitals without changing the position of the s and p states. Figure 2 shows the chemical shift of oxygen in CaO as a function of this level shift of the Ca 3d state in the isolated Ca^{2+} ion (used to generate the pseudopotential). This figure clearly shows that the energy position of the 3d state of Ca has a strong influence on the ^{17}O chemical shift.

From this observation, we hypothesize that the PBE-DFT error in the ^{17}O chemical shifts is due to an error in the PBE-DFT position of the Ca 3d levels with respect to the O 2p states. By shifting the 3d orbitals by +3.2 eV, the Ca-3d O-2p hybridization is reduced and the computed and measured chemical shifts of CaO coincide. To check if this 3d level shift could be a systematic and transferable correction of the DFT error on the calculated ^{17}O chemical shifts, we recomputed the grossite and wollastonite NMR parameters using the modified

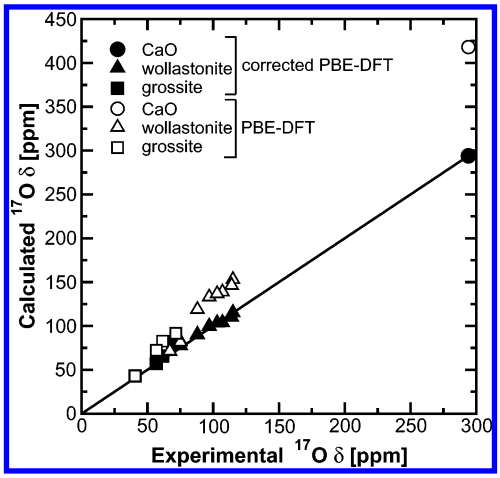

Figure 3. Theoretical ^{17}O chemical shifts as a function of the experimental ones, with the assignment presented in Table 4. Filled and open symbols represent the results obtained with and without the 3d Ca level shift. The line indicates perfect agreement.

Table 5. NMR Parameters of ^{27}Al and ^{29}Si

	PBE-DFT			corrected PBE-DFT		
compound	δ	Cq	η	δ	Cq	η
grossite (^{27}Al)	72.6	6.92	0.79	73.5	6.93	0.79
	68.44	9.95	0.74	68.9	9.97	0.74
wollastonite (^{29}Si)	−91.4			−89.6		
	−91.2			−89.6		
	−89.0			−87.3		

[a] We report the results obtained with (corrected PBE-DFT) and without (PBE-DFT) the shift in the energy of Ca 3d level.

Table 6. Experimental and Relaxed PBE-DFT Volumes in Bohr^3 of CaO and MgO

compound	experimental	PBE-DFT	corrected PBE-DFT
CaO	187.2	190.36(+1.7%)	198.4(+5.9%)
MgO	126.5	131.7(+4.1%)	

[a] In parenthesis we indicate the deviation of the theoretical values from the experimental ones. we report the results obtained with (corrected PBE-DFT) and without (PBE-DFT) the shift in the energy of Ca 3d level.

pseudopotential, optimized for CaO. The results, presented in Table 4, show a very good agreement with the experimental values, in contrast to our previous results. A summary of these results is also presented in Figure 3, where the values of the calculated chemical shifts are plotted against the corresponding experimental values. Given the diversity of the Ca and O environments in the different structures, we are able to conclude that the correction is indeed transferable.

We notice that only the NMR chemical shifts of ^{17}O are influenced by the 3d Ca level shift. The effect of the 3d shift on the ^{17}O electric field gradient is negligible, as shown in Table 4, as it is on the NMR parameters of the other atoms such as Si and Al, as shown in Table 5. The forces on the atoms are also not affected by the level shift. Indeed, the largest difference between the forces computed with the standard and the corrected Ca pseudopotential on the atoms of the grossite and wollastonite is 0.004 Ry/au. In Table 6, we show the influence of the correction on the equilibrium volume of the CaO and MgO structure. Here the influence of the correction is not negligible. However, the overestimation of the volume by the calculation with the shifted Ca 3d level is the expected one from the use of GGA-PBE. Indeed, GGA-PBE usually overestimates the bond lengths by 1−2% and the equilibrium volumes by 3−6%.[33]

Table 7. Transverse Optical Phonon Frequency (THz) at the Γ Point of CaO and MgO[a]

compound	experimental	PBE-DFT	corrected PBE-DFT
CaO	9.05	8.52	10.41
MgO	12.23	12.55	

[a] We report the results obtained with (corrected PBE-DFT) and without (PBE-DFT) the shift in the energy of Ca 3d level. The calculations are performed at the experimental lattice constant. The phonon frequencies are obtained from the force computed on the O atom when the O is slightly displaced along the crystallographic (111) direction. The experimental frequencies are taken from ref 34.

Finally, to investigate the effect of the 3d level shift on other response properties, we compute, for CaO and MgO, the transverse optical phonon frequency at the Γ point, using the experimental lattice constant. The results are reported in Table 7. Whereas in MgO the theoretical GGA-PBE frequency overestimates the experimental one, in CaO the GGA-PBE frequency is smaller than the corresponding experimental value. This contrasting behavior could be due to the position of the 3d of Ca within GGA-PBE. The lower the 3d levels are, the larger the dielectric screening is due to virtual transitions involving the 3d states, and the lower the phonon frequency is. Indeed, by shifting the 3d levels up in energy, the phonon frequency increases. However, the shift optimized for the NMR calculations overcorrects the phonon frequency, and the result obtained with the shifted 3d levels is worse than that obtained with the original GGA-PBE functional.

Assignments

The accuracy of the corrected chemical shifts makes it possible to assign the experimental parameters to the different oxygen sites in grossite and wollastonite. In grossite, the O1 site can be identified by its multiplicity, which is different from that of the other sites. The calculations allow us to assign the O2 and O3 and O4 sites, as reported in Table 4. In particular we confirm the interpretation of ref 4 that assigned the site O4 to the tricluster.

For wollastonite, we can assign nearly all of the oxygen sites using both the chemical shift and the value of Pq (which is the only quadrupolar parameter determined experimentally in the present study).

In Figure 4, we present, in a two-dimensional (δ,Pq) space, the measured and computed NMR parameters for each O site of wollastonite. We assign the experimental spectra by minimizing

$$\chi^2 = \frac{1}{2N}\sum_{i=1}^{N}\left[\frac{(\delta_i^{\text{exptl}} - \delta_i^{\text{theor}})^2}{2\Delta\delta^2} + \frac{(Pq_i^{\text{exptl}} - Pq_i^{\text{theor}})^2}{2\Delta Pq^2}\right] \quad (5)$$

as a function of the assignment. Here N is the number of sites, the superscript distinguishes experimental and theoretical quantities, and $\Delta\delta$ and ΔPq are the declared uncertainties in the experimental results, equal to 2 ppm and 0.2 MHz, respectively. The lowest χ assignment is reported in Figure 4 and in Table

(32) *Zahlenwerte und Funktionen aus Naturwissenschaften und Technik*; Madelung, O., Ed.; Springer: New York, 1982; Landolt-Bornstein, New Series, Group III, Vol. 17b.
(33) For example, see: Hamann, D. R. *Phys. Rev. Lett.* **1996**, *76*, 660 and references therein.

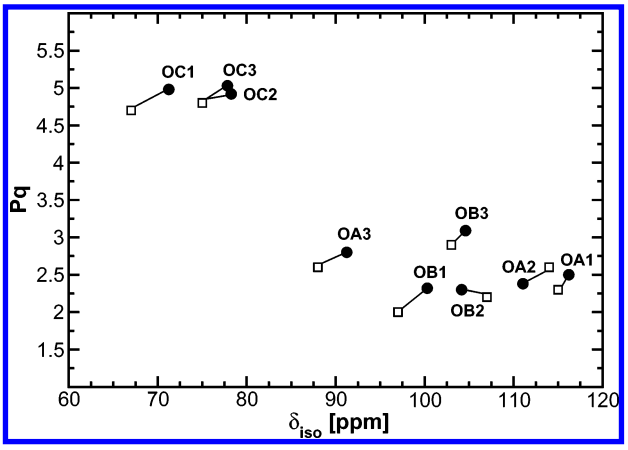

Figure 4. Assignment of the wollastonite ^{17}O spectra. Empty squares represent the experimental points, whereas full circles represent the calculated ones.

Table 8. Calculated and Experimental NMR Parameters of ^{27}Al in Grossite and ^{29}Si in Wollastonite[a]

	experiment			corrected PBE-DFT			
compound	δ	Cq	η	δ	Cq	η	assign.
grossite (^{27}Al)	76.0	6.25	0.88	73.5	6.93	0.79	Al1
exptl ref 35	70.0	9.55	0.80	68.9	9.97	0.74	Al2
grossite (^{27}Al)	68.1	6.4	0.90				
expt ref 36	59.1	9.5	0.82				
wollastonite (^{29}Si)	−91.7			−89.6			Si1
	−91.7			−89.6			Si2
	−87.6			−87.3			Si3

[a] For the calculated values we use the corrected PBE-DFT Hamiltonian with shifted 3d Ca orbitals. For grossite two different sets of experimental data are reported.[35,36] The assignment is labeled with the same convention used in the description of the crystalline structures.[29,30]

4. However, a very similar χ is obtained by interchanging the assignment of the OA1 and OA2 sites, which are too close to be clearly distinguished.

In Table 8, we compare the experimental and theoretical ^{27}Al and ^{29}Si and NMR parameters of grossite and wollastonite. In this case as well, we can assign the different crystallographic sites, by comparing the experimental and theoretical NMR parameters. For grossite, two sets of experimental data are available in the literature.[35,36] Our calculations agree more closely with the data of ref 35.

Theoretical Context

In this work, we approach the deficiencies of PBE-DFT in the description of the Ca 3d level and hence (as shown by our calculations) the ^{17}O chemical shifts, in an empirical manner, by shifting the energy of the Ca 3d levels by a constant value. The 3d energy shift is a transferable correction, which works in different chemical environments. In addition, the 3d energy shift does not affect the other properties which are well treated in PBE-DFT. We now place these observations within the context of the current understanding of the limitations of DFT.

It is well-known that current implementations of DFT (in particular the LDA and various types of GGAs) do not give the correct excited-state spectrum. In the solid state this error is referred to as the "band gap problem" and is present for all

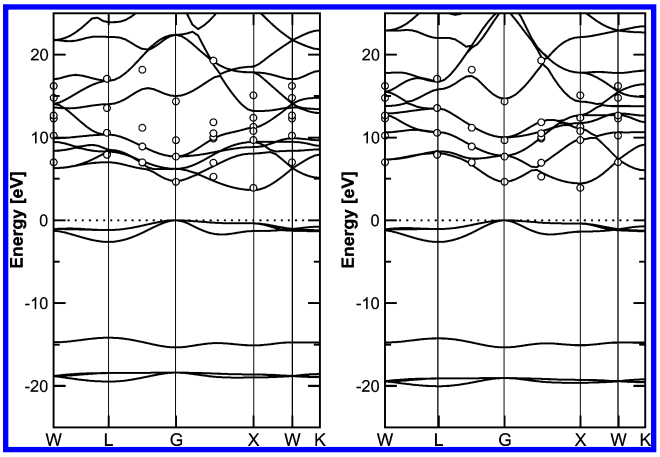

Figure 5. Band structure of CaO. The pure PBE-DFT result (left) and the PBE-DFT result with the Ca 3d level shifted by +3.2 eV (right). The open circles are the GW results of Yamasaki and Fujiwara[39] for the conduction band, shifted by −2.68 eV.

insulators. While in many cases this error can be approximated by a rigid upward shift in energy of the unoccupied states (the "scissor operator"),[37,38] the situation can be more complex. Localized orbitals, such as the Ca 3d of our case, can be differently shifted in energy as compared to the other bands. This relative shift significantly affects the degree of hybridization of these localized states with others. This in turn affects the response properties, for example effective charges[16] or chemical shifts. As experience shows that the calculated chemical shifts of insulators are generally in good agreement with experiment, but the "band gap error" is always present, it is clearly the relative shift of the localized orbitals that is responsible for the apparent breakdown of DFT seen in this work.

Ab initio excited spectra that agree well with experimental ones can be calculated using the GW method. Yamasaki and Fujiwara[39] have performed just such a calculation for CaO (and other metal oxides). Comparing our band structures, calculated using the modified Ca potential, with those of ref 39, we find generally good agreement (Figure 5), with the exception of a rigid shift of 2.68 eV. This difference in the band gap is not surprising as our modification of the Ca pseudopotential can only affect the 3d levels. Otherwise the form of the band structures are very similar. The bandwidths and relative positions of the conduction bands match well. This reconciles our apparent success with our level-shifting approach's empirical nature. The calculations performed using the modified Ca potential have effectively been done at a higher level of theory than PBE-DFT, hence the improved accuracy. We note that it would have been feasible to find a shift of the Ca 3d level by reference to the GW calculation alone; our method would then be fully ab initio. However, a more convenient, self-consistent approach would be to use self-interaction corrected (SIC) pseudopotentials.[40] A related level-shifting approach is familiar to the quantum chemical community.[41] However, while this approach improves over DFT in small molecules, it is not appropriate in

(34) Schütt, O.; Pavone, P.; Windl, W.; Karch, K.; Strauch, D. *Phys. Rev. B* **1994,** *50*, 3746.
(35) Stebbins, J. F.; Oglesby, J. V.; Kroeker, S. *Am. Miner.* **2001**, *86*, 1307−1311.
(36) Gervais, C.; MacKenzie, K. J. D.; Smith, M. E. *Magn. Res. Chem.* **2001**, *39*, 23.
(37) Levine, Z. H.; Allan, D. C. *Phys. Rev. Lett.* **1989**, *63*, 1719.
(38) Gonze, X.; Ghosez, Ph.; Godby, R. W. *Phys. Rev. Lett.* **1995**, *74*, 4035−4038.
(39) Yamasaki, A.; Fujiwara, T. *Phys. Rev. B* **2002**, *66*, 245108.
(40) Filippetti, A.; Spaldin, N. A. *Phys. Rev. B* **2003**, *67*, 125109.
(41) Malkin, V. G.; Malkina, O. L.; Casida, M. E.; Salahub, D. R. *J. Am. Chem. Soc.* **1995**, *116*, 5898.

Table 9. Dependence of the ^{17}O δ (ppm) on the Metal Ion and on the Unit Cell Volume in the Simple Oxides[a]

metal	unit cell volume	^{17}O δ (ppm)
corrected Ca	CaO volume	294.0
Ca_{3dMg}	CaO volume	81.7
Mg	CaO volume	99.8
Mg	MgO volume	58.8

[a] In Ca_{3dMg} the 3d Ca orbitals in the +2 ionic configuration are displaced to the energy level of the 3d Mg orbitals.

the solid state. Indeed, the level energy shift defined in ref 41 vanishes in extended periodic systems, where the eigenstates are Bloch states, extended over all space.

Oxygen−Alkaline-Earth Metals Interaction

As discussed in the Introduction, the chemical shifts of O sites close to alkaline-earth metals depend critically on the species of the metal atom. This dependence can have three possible origins. (i) The hybridization of the empty d orbitals of the alkaline-earth ion with the 2p O orbitals, as discussed in previous sections. (ii) The interaction of the s and p orbitals of the alkaline-earth ion with the O orbitals. The $3s^2$ and $3p^6$ orbitals of Ca have a larger spatial extent than the Mg $2s^2$ and $2p^6$ orbitals. Thus for a given metal ion−O distance, the electrostatic and Pauli repulsion between the electrons in the O orbitals and the electrons in the metal ion orbitals are larger for Ca than for Mg. Moreover the empty 4s and 4p states of Ca have a higher energy than the empty 3s and 3p states of Mg. As a result, the hybridization of O orbitals with the s and p states of the metal ion is different for Mg and Ca. (iii) The distance between the metal ion and the O atom, which varies with the alkaline-earth ionic radius.

To study the effect of the hybridization, we generated a Ca pseudo-atom, which we call Ca_{3dMg}, in which the energy of 3d orbitals in the isolated Ca^{2+} ion are placed at the same level as the 3d orbitals in the isolated Mg^{2+} ion. In this case, the Ca^{2+} 3d orbitals are shifted with respect to the PBE-DFT position by +8.96 eV. The occupied Ca^{2+} states are not modified by the shift.

By replacing a Ca pseudo-atom with a Ca_{3dMg} pseudo-atom, we artificially suppress the hybridization of 3d Ca states with the 2p O orbitals, without modifying the occupied and empty s and p Ca states.

To decouple the three different effects in the simple oxides, we compare in Table 9 the results for CaO and MgO, which we presented in the previous sections, with those obtained for $Ca_{3dMg}O$ using the experimental CaO volume and those obtained for MgO using the experimental CaO volume.

From these data, we notice that the 3d hybridization is the dominant effect: the displacement of the 3d states in CaO results in an increase of the shielding of 212 ppm. The replacement of $Ca_{3dMg}O$ with MgO at constant volume, i.e., the modification of the s and p states of the metal, accounts for a small deshielding of 18 ppm. The reduction of the volume in MgO from that of CaO to that of MgO, i.e., the effect of the geometry, results in a shielding of 41 ppm.

We use a similar approach to study the effect of the Ca−Mg substitution on the nonbridging oxygens of silicates. Experimentally the Ca−Mg substitution results in a larger shielding of about 65 ppm.[5,18,19] From the result obtained from the simple oxides, we assume that the effect of the geometry on the ^{17}O δ is minor, and we replace, in the wollastonite structure, the Ca atoms with Ca_{3dMg} atoms or with Mg atoms. The calculated chemical shifts are reported in Table 10. The Ca−Ca_{3dMg} replacement results in an average increase in the shielding of 49 ppm for the six nonbridging oxygens (OA1−OB3). The Ca−Mg replacement results in an average increase in the shielding of 51.24 ppm. Again, in this case, the shifts obtained with Ca_{3dMg} and Mg are very similar, and the hybridization between the 3d Ca and the 2p O states alone accounts for most of the experimentally observed sensitivity of the nonbridging oxygens to the alkaline-earth-metal substitution.

Finally it is interesting to analyze how the hybridization with Ca 3d orbitals influences the O chemical shifts. To decompose the O shielding tensor in an atomic diamagnetic and paramagnetic contribution, we use the symmetric gauge for the vector potential, we center the gauge origin on the O, and we consider only the shielding coming from the induced currents around the O atom. By definition, the diamagnetic contribution of the shielding tensor, $\vec{\sigma}_d$ is given by

$$\vec{\sigma}_d \cdot \mathbf{B} = \frac{1}{c^2} \int d^3r \rho^O(\mathbf{r}) \mathbf{A}(\mathbf{r}) \times \frac{\mathbf{r}}{r^3} \tag{6}$$

where $\boldsymbol{A}(\mathbf{r}) = \boldsymbol{B} \times \mathbf{r}/(2c)$, c is the speed of light, $\rho^O(\mathbf{r})$ is the electron density of the O atom, and the origin coincides with the O position (we use Gauss and atomic units). The paramagnetic contribution can be expressed in terms of virtual transitions between the occupied and empty levels. To evaluate $\rho^O(\mathbf{r})$, we use the PAW method:

$$\rho^O(\mathbf{r}) = 2 \sum_o \left| \sum_n \langle \boldsymbol{r} | \phi_n \rangle \langle \tilde{p}_n | \tilde{\Psi}_o \rangle \right|^2 \tag{7}$$

where $|\tilde{\Psi}_o\rangle$ are the pseudopotential-occupied Kohn−Sham orbitals, $\langle \tilde{p}_n|$ and $|\phi_n\rangle$ are the PAW O projector functions and O all-electron partial waves, respectively, as defined in ref 9.

To study the effect of the 3d Ca hybridization on the diamagnetic part of the shielding tensor, we replace in the CaO and the wollastonite structures the Ca atoms (described by the corrected-PBE pseudopotential) by Mg atoms, without modifying the geometry. The absolute variations of σ_d are smaller than 2 ppm. Given the much larger variation of the ^{17}O total chemical shift with the Ca−Mg substitution (see Tables 9 and 10), we

Table 10. Dependence of the ^{17}O δ on the Metal Ion in Wollastonite[a]

	^{17}O chemical shift (ppm)								
metal	OA1	OA2	OA3	OB1	OB2	OB3	OC1	OC2	OC3
corrected Ca	115.29	110.09	90.33	99.74	103.89	103.51	70.95	78.04	77.62
Ca_{3dMg}	59.69	56.44	46.68	56.20	55.33	55.12	69.93	72.14	72.25
Mg	59.60	58.01	51.17	47.32	35.34	63.91	74.66	70.46	70.05

[a] The calculations are performed with the experimental structure of the Ca silicate.[30] In Ca_{3dMg} the 3d Ca orbitals in the +2 ionic configuration are displaced to the energy level of the 3d Mg orbitals.

conclude that the sensitivity of the O NMR chemical shifts on the 3d Ca hybridization is not due to a variation of the ground-state electron density but to the variation of the paramagnetic contribution to the shielding, which involves transitions between occupied and virtual states.

Conclusion

Contrary to our expectations, we find that the PBE-DFT is not sufficiently accurate for the description of Ca aluminosilicate systems. This deficiency is traced to the incorrect treatment of the unoccupied Ca 3d level by PBE-DFT. In particular we find that the ^{17}O chemical shifts are very sensitive to the hybridization between the O 2p orbitals and the 3d orbitals of neighboring Ca atoms. In the PBE approximation, the energy of Ca 3d orbitals is too low and the hybridization with O 2p orbitals is overestimated.

It is possible to correct for this deficiency in a simple way by shifting the Ca 3d energy by a constant value of +3.2 eV. For the prediction of NMR chemical shifts, the correction is transferable, since the same shift works well for very different chemical environments. The 3d level shift has a little influence on ^{17}O electric field gradients or on the NMR parameters of other nuclei like ^{27}Al or ^{29}Si. The 3d level shift has an impact on the phonon frequencies, but the correction optimized for the prediction of the NMR parameters is not appropriate for the phonon calculation.

The accuracy of chemical shift calculations, obtained with the shifted 3d levels, allows us to assign the different oxygen sites in Ca-containing crystalline structures. This at once clearly demonstrates the limitations of DFT for the calculation of NMR chemical shifts, indicates when they may manifest themselves, and suggests a remedy.

The partially covalent nature of the Ca−O bond, which is absent in the purely ionic Mg−O bond, has an impressive influence on the ^{17}O chemical shifts. Indeed, we show that Ca 3d O 2p hybridization alone can explain why in Ca oxides and aluminosilicates the ^{17}O chemical shifts are much more deshielded than those of the corresponding Mg compounds. Such a deshielding is not due to a decrease in the ground-state charge of O but to an increase of the paramagnetic response due to virtual transitions involving the Ca 3d orbitals.

We expect that what we observe in Mg and Ca compounds can be generalized to the other alkaline and alkaline-earth oxides and aluminosilicates. In particular, our results suggest that the hybridization between the lowest unoccupied *n*d state of the metal and the 2p of the O explains the dependence of ^{17}O chemical shifts on the species of the alkaline or alkaline-earth atom.

In a recent paper,[42] Tossell found a strong dependence of the ^{17}O chemical shifts of alkaline-earth oxides on the *d* functions of the metal basis set. This observation supports (without quantifying it) the crucial role of the metal *n*d state in the ^{17}O chemical shifts. The results in ref 42 were obtained with the B3LYP-hybrid-DFT functional and with Hartree−Fock (HF). B3LYP overestimates the effect of Ca−Mg substitution on the ^{17}O chemical shifts by 54 ppm.[42] We recall that the overestimation obtained in the present paper for the PBE-DFT functional is even larger (124 ppm). HF underestimates the effect of Ca−Mg substitution by 38 ppm.[42] Thus the smaller error of B3LYP compared to that of PBE can be explained by the presence of the exact HF exchange in the B3LYP functional.

Acknowledgment. The calculations have been carried out on IBM SP3 and SP4 in the French CNRS computer center IDRIS in Orsay using the PARATEC code.[43] The work of C.J.P. was supported by the EPSRC. We thank Atsushi Yamasaki for the GW data.

JA0490830

(42) Tossell, J. A. *Phys. Chem. Miner.* **2004**, *31*, 41.
(43) Pfrommer, B.; Raczkowski, D.; Canning, A.; Louie, S. G. PARAllel Total Energy Code. With contributions from Mauri, F.; Cote, M.; Yoon, Y.; Pickard, C.; Haynes, P.